PHILOSOPHICAL TRANSACTIONS OF THE ROYAL SOCIETY A MATHEMATICAL, PHYSICAL & ENGINEERING SCIENCES

Scanning Acoustic Microscopy of Partly Embedded Cracks in Polycrystalline Alumina

G. C. Smith, E. A. Almond, M. G. Gee and M. Nikoonahad

Phil. Trans. R. Soc. Lond. A 1986 **320**, 237-241
doi: 10.1098/rsta.1986.0113

Phil. Trans. R. Soc. Lond. A **320**, 237–241 (1986)
Printed in Great Britain

Scanning acoustic microscopy of partly embedded cracks in polycrystalline alumina

By G. C. Smith[1], E. A. Almond[1], M. G. Gee[1] and M. Nikoonahad[2]†

[1] *Division of Materials Applications, National Physical Laboratory, Teddington, Middlesex TW11 0LW, U.K.*

[2] *Department of Electronic and Electrical Engineering, University College London, Torrington Place, London WC1E 7JE, U.K.*

[Plates 1–4]

Reflection scanning acoustic microscopy (SAM) at 1 GHz has been used to examine artificially induced cracks in alumina samples. The results are compared with the corresponding optical micrographs and scanning electron microscope images. For a sample with a 0.08 μm centre-line average (CLA) surface finish, the SAM working with a 400 μm frame size, showed that a crack that appeared to be about 150 μm in length in the corresponding optical image was, in fact, at least 200 μm in length. For a sample with a good engineering finish of 0.15 μm CLA, the SAM was able to reveal crack detail to a degree comparable with that revealed by an optical microscope working under optimum conditions. On a sample with a highly polished surface it was possible to distinguish between cracks and grain boundaries by using the $V(z)$ response of the SAM, in agreement with theory.

Introduction

Ceramics are increasingly being used as structural engineering materials. Mechanical weakness in these materials can often be traced to surface damage, such as microcracks, which slowly propagate under low loads (in aggressive environments) and cause premature failure. The specification of the surface finish required to avoid failure is difficult because a specification of flatness or roughness does not necessarily exclude the possibility that microcracks may be introduced during the component's preparation. The desirability of a reliable non-destructive evaluation (NDE) technique for inspection of the surface quality of ceramics is therefore evident. Optical microscopy would normally be the first choice, but some ceramics are partly translucent and there are problems in obtaining clear images of surface detail without resorting to coatings. Although scanning electron microscopy (SEM) has intrinsically high spatial resolution, it suffers from the problem of charging of insulating materials and, if useful contrast is to be obtained, the field of view is rather small.

Scanning acoustic microscopy (SAM) is a powerful NDE technique (Nikoonahad 1984*a*) that is potentially suitable for examining these materials. When imaging the surface with a scanning acoustic microscope (Quate *et al.* 1979; Nikoonahad 1984*b*), a tightly focused ultrasonic beam is raster scanned on the surface of the specimen (figure 1). Any surface (or near-surface) elastic discontinuity causes a modulation of the phase and amplitude of the acoustic signal, which is reflected back from the surface. It is this modulation that provides

† Present address: Philips Laboratories, North American Philips Corporation, New York, 10510, U.S.A.

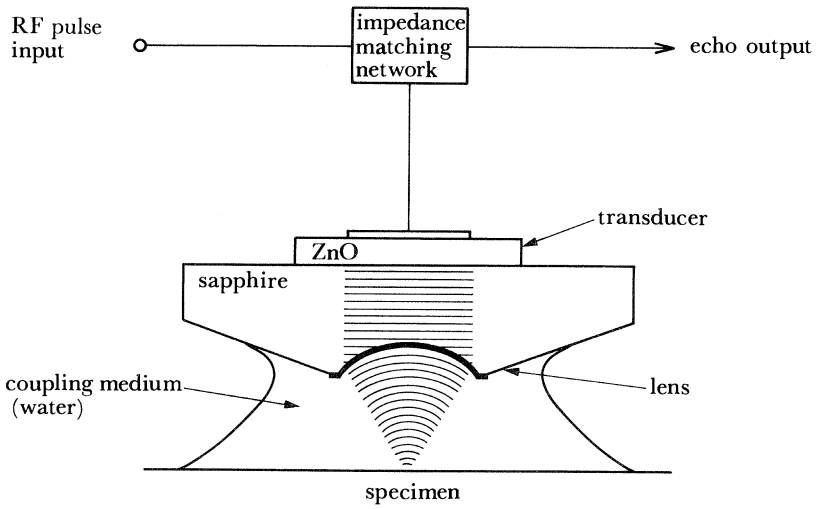

FIGURE 1. Showing the principle of operation of the scanning acoustic microscope.

the contrast in the SAM. Its use for detecting the existence of cracks and defects has already been demonstrated (Yamanaka & Enomoto 1982; Ilett *et al.* 1984). In particular, the variation of transducer output as a function of defocus distance in the acoustic microscope – the $V(z)$ effect – may be used to enhance the detectability of partly embedded microcracks and discontinuities. However, for most of the examples where a particular application of the technique has been demonstrated, the surface finish of the sample was far superior to that required for an average engineering ceramic.

Consequently, the present work was undertaken to investigate the advantages of acoustic over optical microscopy for a selection of surface finishes.

It will be shown that cracks smaller than the resolution of the microscope can be detected and imaged with an SAM for surfaces of ceramics prepared in a routine manner. Also, it will be shown that with an SAM one can distinguish between discontinuities due to grain boundaries and those of partly embedded cracks.

Alumina was chosen as the ceramic for this study because it is widely used industrially both as polycrystalline sintered material, and as single-crystal sapphire. It is elastically and acoustically well characterized (Wachtman *et al.* 1960; Kushibiki *et al.* 1981).

SAMPLES

Three samples of alumina were prepared. Sample A was 95% (by mass) alumina with additions of CaO and SiO_2 and a surface finish of 0.08 μm centre-line average (CLA). This corresponds to a very good engineering finish, rather better than that required for most applications. The top surface was indented with a Vickers pyramid indenter with a load of 196 N, to produce cracks which propagated radially from the corners of the indentation.

The second sample, B, was a piece of the same alumina as sample A, with a good engineering surface finish of 0.15 μm CLA. It was indented with a load of 196 N. The indenter was oriented so that the cracks were parallel and perpendicular to the long axis of the sample. They were propagated by using a bridge loading technique (Warren & Johannesson 1984), which caused

them to grow perpendicular to the indented surface; as a result, they could be viewed either from above, looking at the top surface, or as they emerged at the side of the sample, as shown in figure 2.

Sample C was a wear-test specimen. It was a pin of 99.5% (by mass) alumina, of length 20 mm and diameter 6 mm, that had been held against a wheel of the same alumina for 180 min with a force of 120 N. The wheel was rotated to give a relative speed of 0.37 ms^{-1}. During the test, fracture of the sample occurred and pieces of material splintered off. The sample was subsequently sectioned longitudinally, mounted and polished to 0.04 μm CLA with diamond paste and silica suspension (a good optical finish) to reveal the crack pattern formed during the wear and splintering process.

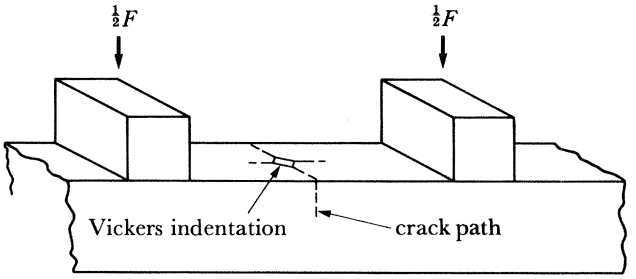

FIGURE 2. Crack pattern produced by propagating the indentation crack in sample B.

RESULTS AND DISCUSSION

All the acoustic micrographs presented in this section were taken at a frequency of 1 GHz with water as the coupling medium. The imaging resolution was therefore about 1 μm.

Figure 3, plate 1, shows an optical micrograph of the corner of the 196 N hardness indentation on specimen A. The sample was illuminated from above in the normal reflection mode, and quite good contrast was obtained from the crack propagating from the corner of the indentation. This crack appears to extend approximately 150 μm from the corner of the indentation. Part of the same area viewed in the acoustic microscope is shown in figure 4. The acoustic lens was focused on the undamaged area of material away from the indentation. The corner of the indentation, and the crack, are clearly seen and the crack appears to extend significantly further than was visible in the optical microscope. The significance of the present observation is that the surface of this specimen is rather rough and is not at all like the optically flat and polished surfaces normally examined in acoustic microscopy studies of this kind.

The amount of crack pattern detail that can be revealed acoustically is illustrated in figure 5*a*, plate 2, which is a composite image formed from several acoustic frames following the main crack from the indentation on the top surface of specimen B. Figure 5*b* shows the corresponding optical image. At several points on the acoustic images the crack can be seen to divide and recombine, apparently as it passes around either side of grains in the material. It also shows a tendency to pass preferentially through pores; indeed, even where a distinct crack is not visible, there appears to be a continuation of the crack trace marked by a line of pores.

It is clear that the optical micrographs show the surface detail to be better resolved but it is easier to follow the crack on the acoustic image; this is not evident from figures 5*a*, *b* because of the superior quality of the optical-microscope camera system.

This sample was also examined in the SEM, and the crack width was found to be 100 nm near the crack tip at a position where it was just detectable in the acoustic microscope.

There are two factors which are thought to be responsible for the detectability of suboptical cracks by using the SAM. First there is the large change in the amplitude of the specularly reflected waves when scanning over a crack. The change in impedance can be as high as a factor of 10^6 for an air-filled crack.

Secondly, a partly embedded crack acts as a strong scatterer of the Rayleigh waves generated by the lens at the interface between the sample and the coupling medium, leading to added contrast. However, surface roughness is also a strong scatterer of Rayleigh waves, and on rough surfaces the $V(z)$ effect is much reduced. The significance of the effect of surface roughness can be seen by comparing the acoustic images from samples A and B with those from sample C which had a good polished surface of 0.04 μm CLA.

An acoustic image of the surface of sample C with the lens at focus is shown in figure 6, plate 3. The main feature is a crack running diagonally from top right to the lower left-hand corner, which can only be partly distinguished in the corresponding optical micrograph, taken with reflection contrast, shown in figure 7.

Figure 8, plate 4, shows the image obtained with the lens 5 μm below focus and, in addition to the contrast from the crack seen in the focused image, a network of fine lines can be seen. From this image it is not clear whether these lines represent additional microcracks or are some other feature, however, when the lens is taken 5 μm above focus further contrast is seen (figure 9). Although the additional network of fine lines has disappeared, areas between the lines show as regions of differing intensity.

The basic theory of the $V(z)$ response and its relation to material parameters has been known for some time (Wickramasinghe 1979; Bertoni 1984). However, recent work has emphasized the modifications to the response, which take place owing to the presence of either cracks or other abrupt discontinuities (Cox & Addison 1984; Somekh *et al.* 1985), or elastic anisotropy (Somekh *et al.* 1984). The phenomenon of grain contrast in the SAM is a result of the random orientation of the elastically anisotropic grains of the polycrystalline sample material. Each grain orientation has its own characteristic $V(z)$ response, and hence an image taken with a fixed value of lens defocus shows contrast from grain to grain, depending on orientation. We therefore identify the regions of differing contrast in figure 9 as grains, and it is clear that the network of fine lines in figure 8 represents grain boundaries. A high-magnification acoustic image of the central area of this region taken with +8 μm defocus clearly reveals that this part of the crack is transgranular (figure 10). Around each microstructural feature there are also fringes characteristic of standing acoustic waves (Yamanaka & Enomoto 1982).

According to recent theoretical work by Somekh *et al.* (1985) the modification to the $V(z)$ response resulting from the presence of an abrupt discontinuity is strongly dependent on the properties of that discontinuity. If the feature is a strong reflector of Rayleigh waves, then the $V(z)$ response is modified in both the positive and negative z-directions. However, if the feature is only weakly reflective then the modifications to the $V(z)$ response only take place in the negative z-region of the curve. No additional contrast is expected in the positive z-region.

These conditions are illustrated by the results from sample C. Comparing figures 6, 8 and 9 shows the crack to be clearly visible in all three regions of $V(z)$ response (negative z, at focus, and positive z) whereas the grain boundaries are only visible in the negative z-regions. Therefore, the crack reflects Rayleigh waves strongly, as expected, and the grain boundaries are only weak reflectors.

PHILOSOPHICAL TRANSACTIONS OF THE ROYAL SOCIETY A MATHEMATICAL, PHYSICAL & ENGINEERING SCIENCES

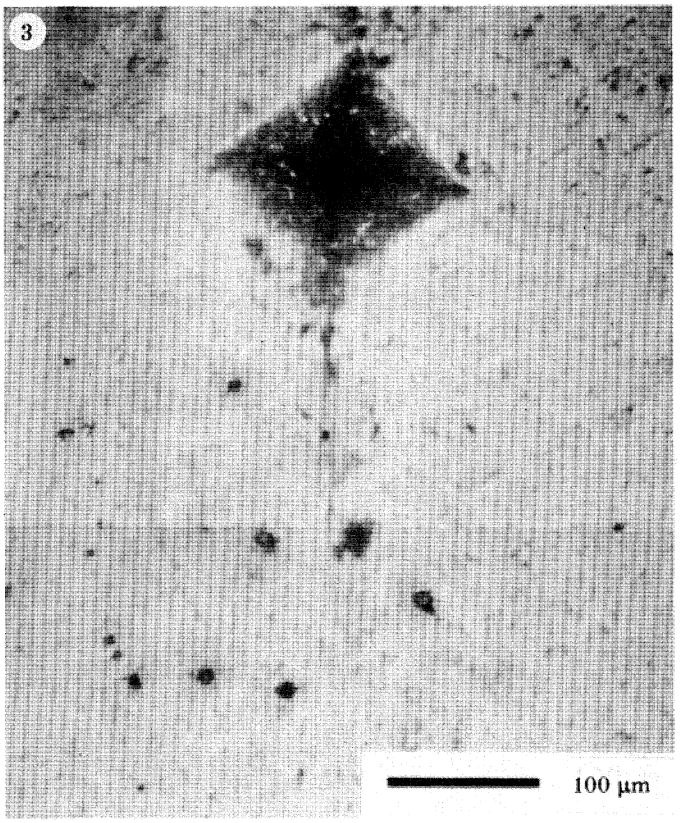

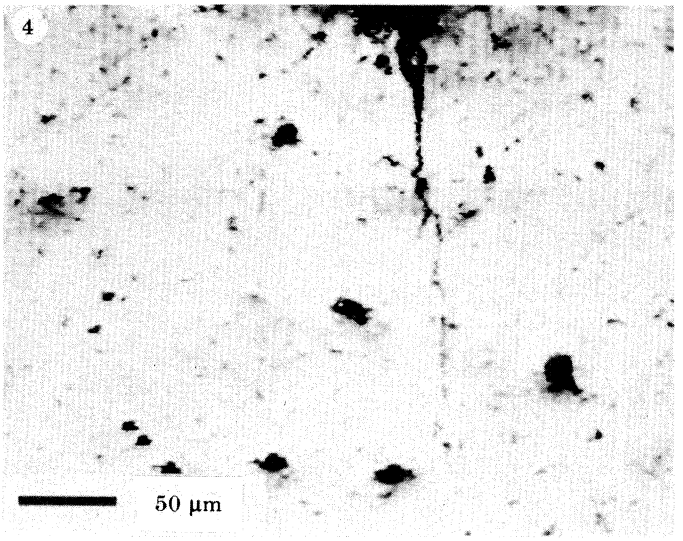

FIGURE 3. Optical micrograph taken in reflection, showing the crack from a corner of the micro-hardness indentation in sample A.

FIGURE 4. Acoustic image corresponding to the same area of sample A seen optically in figure 3.

(*Facing p.* 240)

PHILOSOPHICAL TRANSACTIONS OF THE ROYAL SOCIETY A MATHEMATICAL, PHYSICAL & ENGINEERING SCIENCES

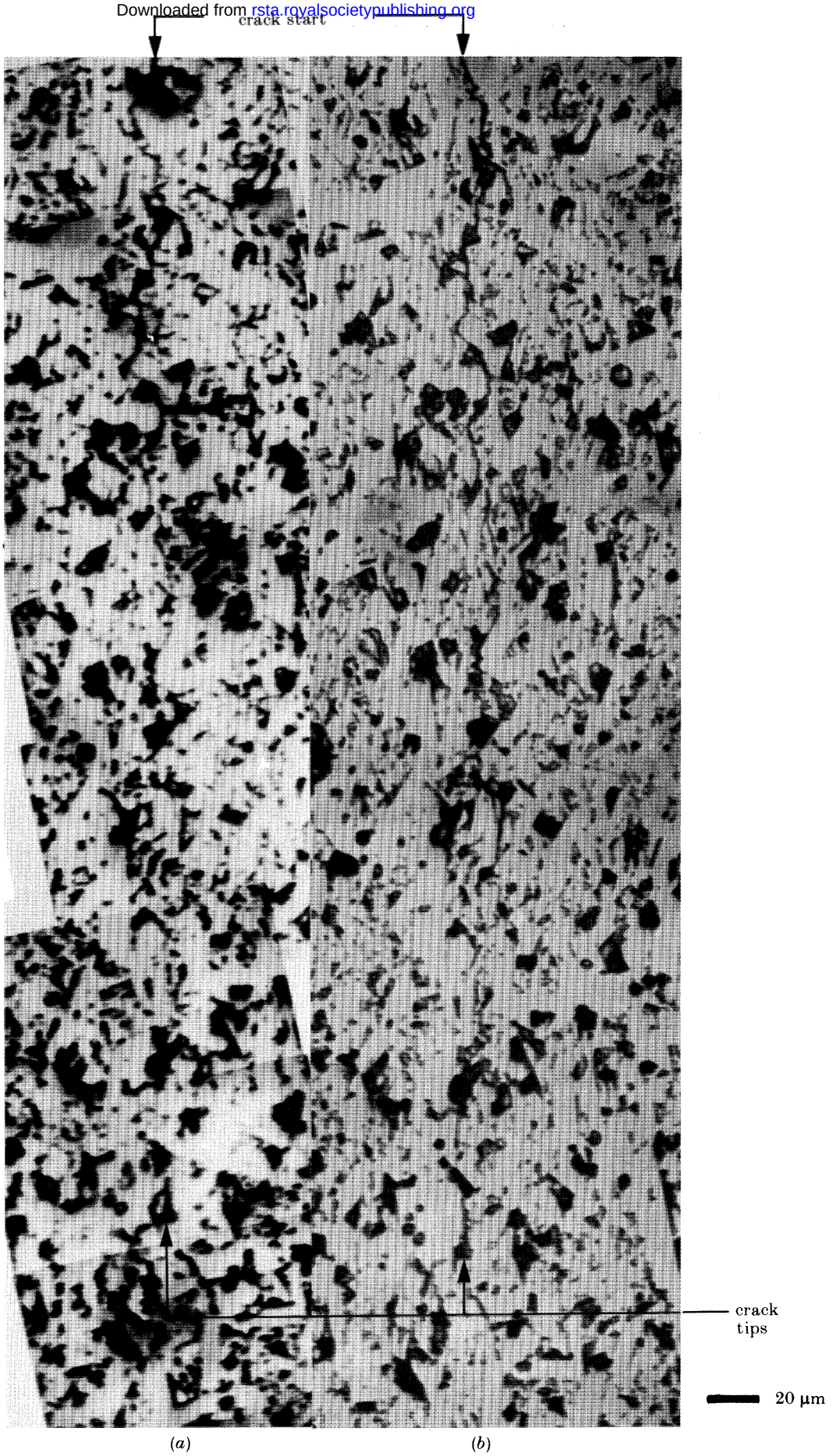

FIGURE 5. (*a*) Composite acoustic image showing the main top surface crack from the indentation on sample B. (*b*) Composite optical image corresponding to the area of sample B shown in (*a*).

PHILOSOPHICAL TRANSACTIONS OF THE ROYAL SOCIETY A MATHEMATICAL, PHYSICAL & ENGINEERING SCIENCES

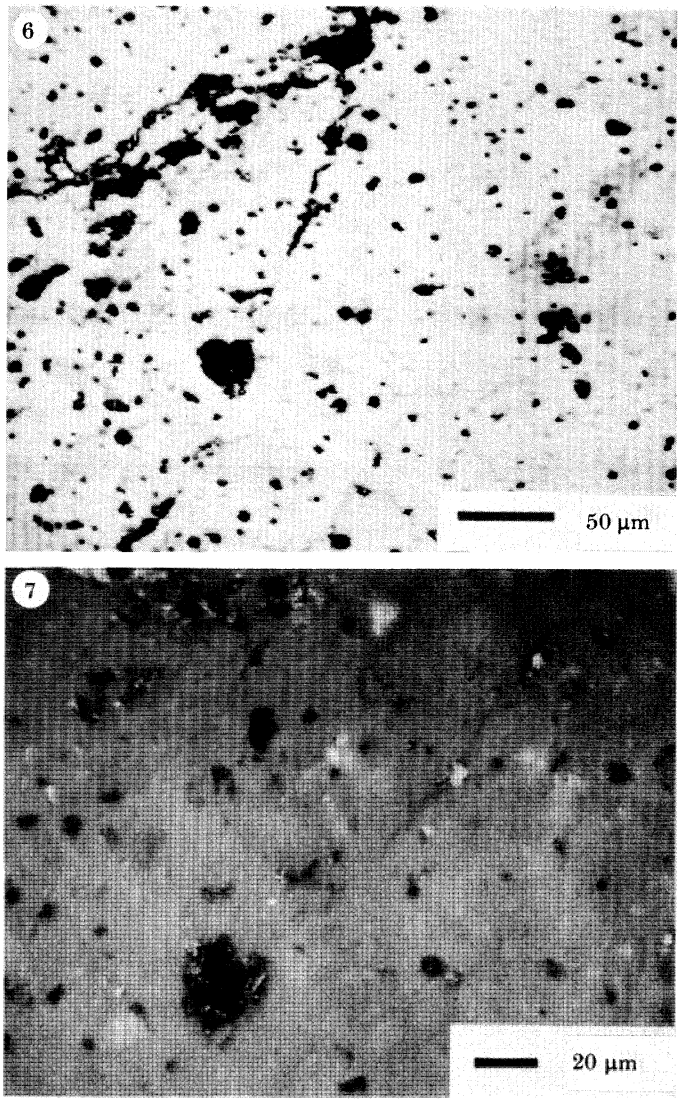

FIGURE 6. Acoustic image of the damage region of sample C showing a fine crack running diagonally from top right to lower left. Taken with the lens at focus ($z = 0$).

FIGURE 7. Optical image taken in reflection, corresponding to the area shown acoustically in figure 6.

PHILOSOPHICAL TRANSACTIONS OF THE ROYAL SOCIETY A MATHEMATICAL, PHYSICAL & ENGINEERING SCIENCES

PHILOSOPHICAL TRANSACTIONS OF THE ROYAL SOCIETY A MATHEMATICAL, PHYSICAL & ENGINEERING SCIENCES

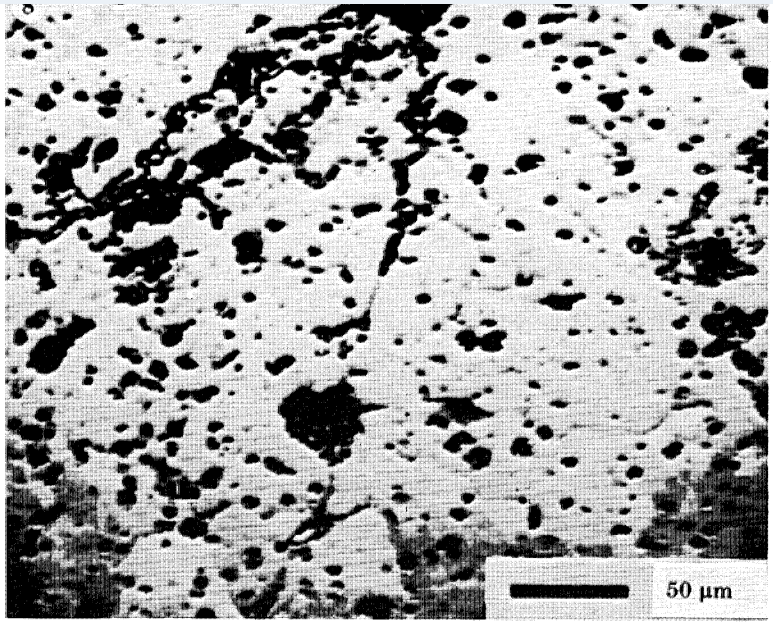

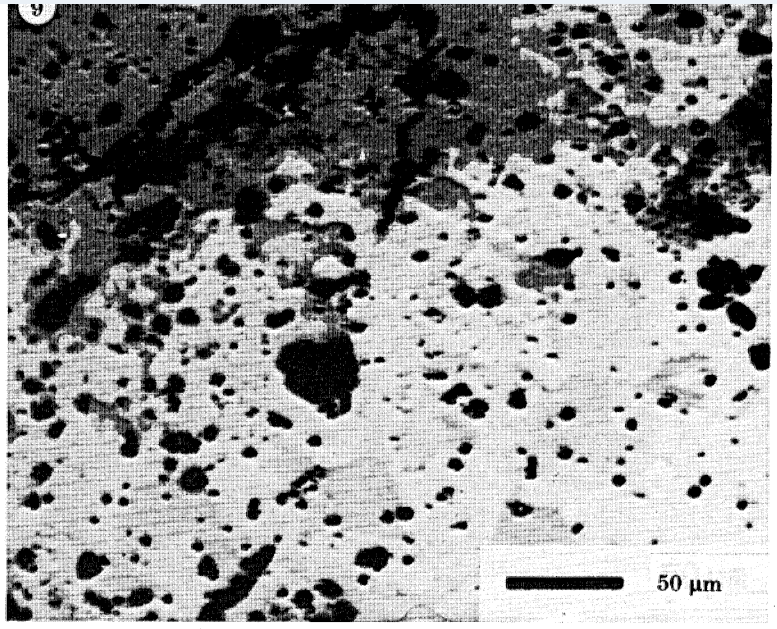

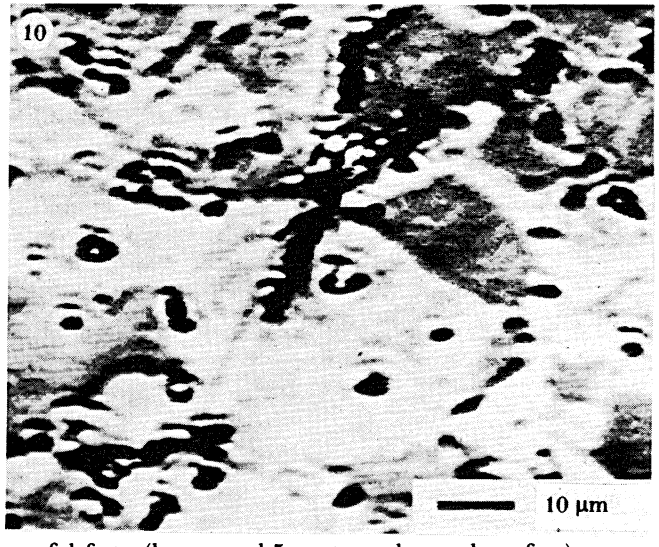

FIGURE 8. Acoustic image taken with $z = -5$ μm of defocus (lens moved 5 μm towards sample surface), corresponding to same area of sample C shown in figure 6.

FIGURE 9. Acoustic image taken with $z = +5$ μm of defocus (lens moved 5 μm away from sample surface), corresponding to area of sample C showing in figure 6.

FIGURE 10. Acoustic image taken with $z = +8$ μm defocus of the central area of sample C shown in figure 6.

Conclusions

We have shown that the SAM is an NDE technique that is directly applicable to examination of cracks in alumina ceramics having a range of surface finishes. For sample B, which had a good engineering finish, the SAM readily provided high-contrast images of a crack that could only be seen by using an optical microscope under optimum conditions.

When the optical and acoustic microscopes were used to image the same area of sample A at low magnification, the crack was significantly clearer in the SAM image. Thus the SAM may often be the more useful instrument to use when scanning for cracks over large areas.

For the highly polished specimen C, where Rayleigh wave scattering by surface roughness was insignificant, we have shown qualitatively that it is possible to distinguish weakly reflective discontinuities (grain boundaries) from strongly reflective features such as cracks. This was done by using the characteristic $V(z)$ response and shows results that are in agreement with recent theory.

We are grateful to Professor E. A. Ash, F.R.S., for his interest and encouragement in this study.

References

Bertoni, H. L. 1984 *IEEE Trans. Sonics Ultrasonics* **SU-31**, 105–116.
Cox, B. N. & Addison, R. C. 1984 *Rev. Progr. Quant. N.D.E.* **3B**, 1173–1184.
Ilett, C., Somekh, M. G. & Briggs, G. A. D. 1984 *Proc. R. Soc. Lond.* A **393**, 171–183.
Kushibiki, J., Ohkubo, A. & Chubachi, N. 1981 *Electron. Lett.* **17**, 534–536.
Nikoonahad, M. 1984*a* Reflection acoustic microscopy for industrial N.D.E. In *Research techniques in nondestructive testing*, vol. 7 (ed. R. S. Sharpe), pp. 217–257. London: Academic Press.
Nikoonahad, M. 1984*b* *Contemp. Phys.* **25**, 129–158.
Quate, C. F., Atalar, A. & Wickramasinghe, H. K. 1979 *Proc. Inst. elect. Electron. Engrs* **67**, 1092–1114.
Somekh, M. G., Bertoni, H. L., Briggs, G. A. D. & Burton, N. J. 1985 *Proc. R. Soc. Lond.* A **401**, 29–51.
Somekh, M. G., Briggs, G. A. D. & Ilett, C. 1984 *Phil. Mag.* **49**, 179–204.
Wachtman, J. B., Jr, Tefft, W. E., Lam, D. G., Jr & Stinchfield, R. P. 1960 *J. Res. natn. Bur. Stand.* **64A**, 213–228.
Warren, R. & Johannesson, B. 1984 *Powder Metall.* **27**, 25–29.
Wickramasinghe, H. K. 1978 *Electron. Lett.* **14**, 305.
Yamanaka, K. & Enomoto, Y. 1982 *J. appl. Phys.* **53**, 846–850.

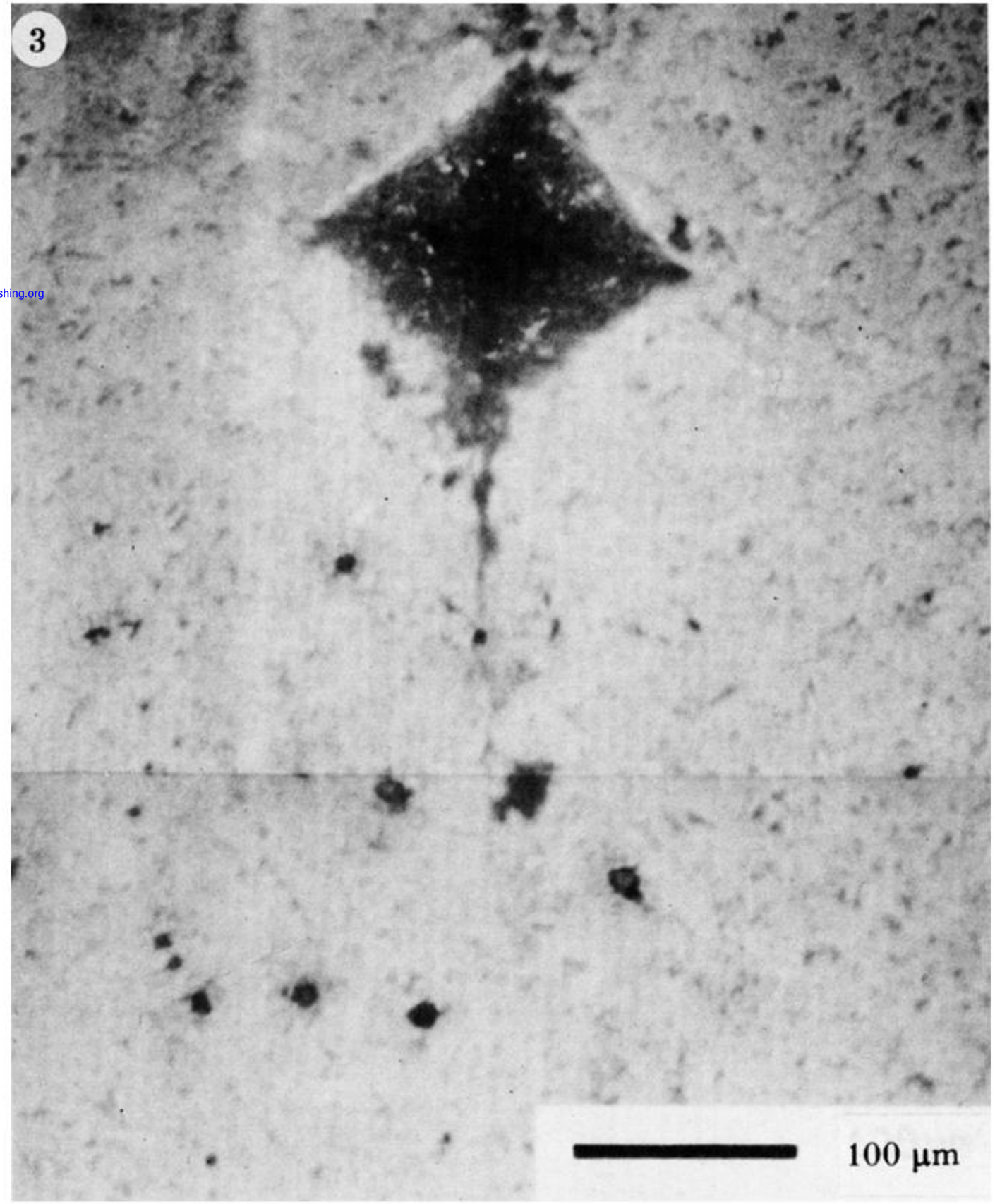

FIGURE 3. Optical micrograph taken in reflection, showing the crack from a corner of the micro-hardness indentation in sample A.

PHILOSOPHICAL TRANSACTIONS OF THE ROYAL SOCIETY A MATHEMATICAL, PHYSICAL & ENGINEERING SCIENCES

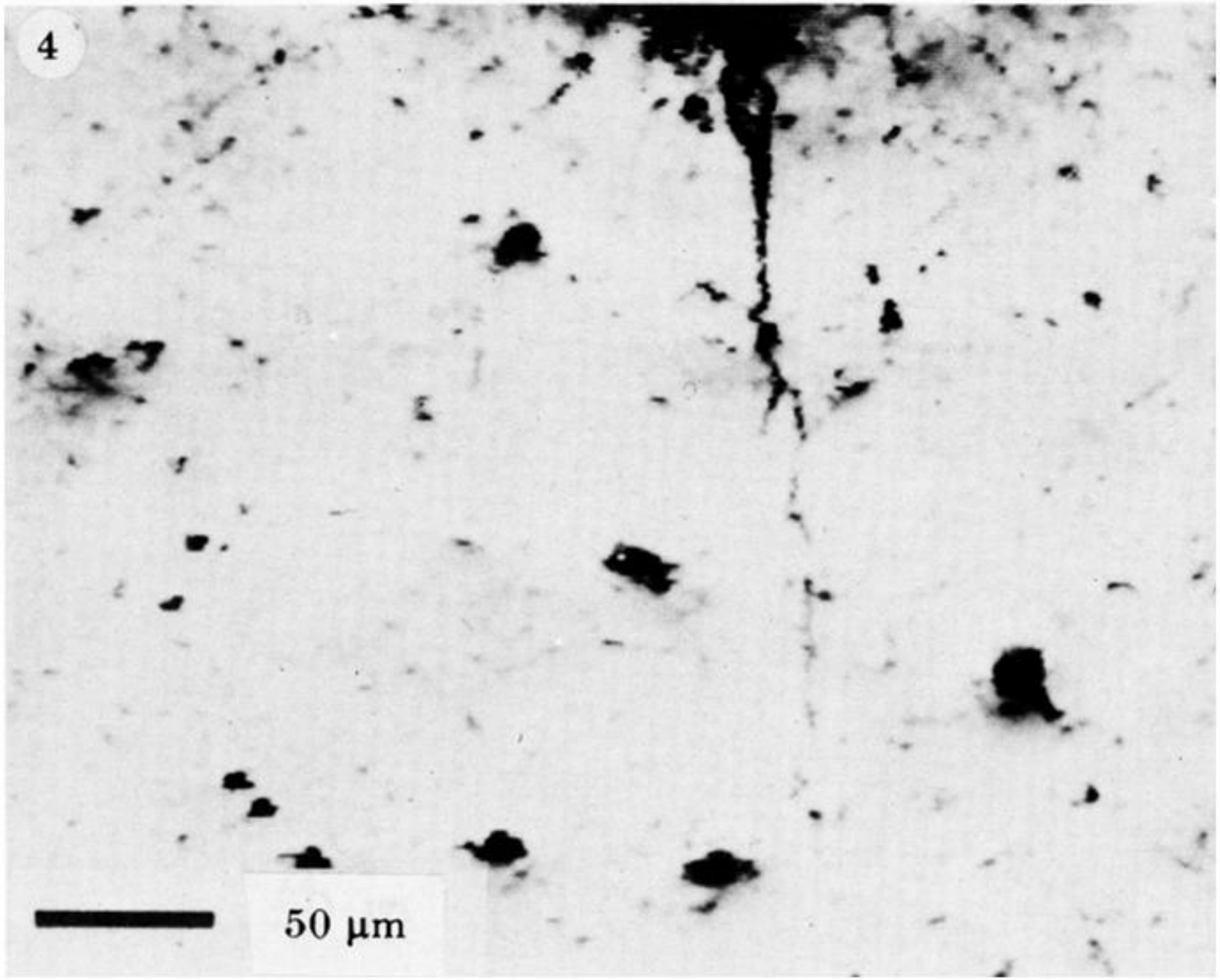

FIGURE 4. Acoustic image corresponding to the same area of sample A seen optically in figure 3.

PHILOSOPHICAL TRANSACTIONS OF THE ROYAL SOCIETY A MATHEMATICAL, PHYSICAL & ENGINEERING SCIENCES

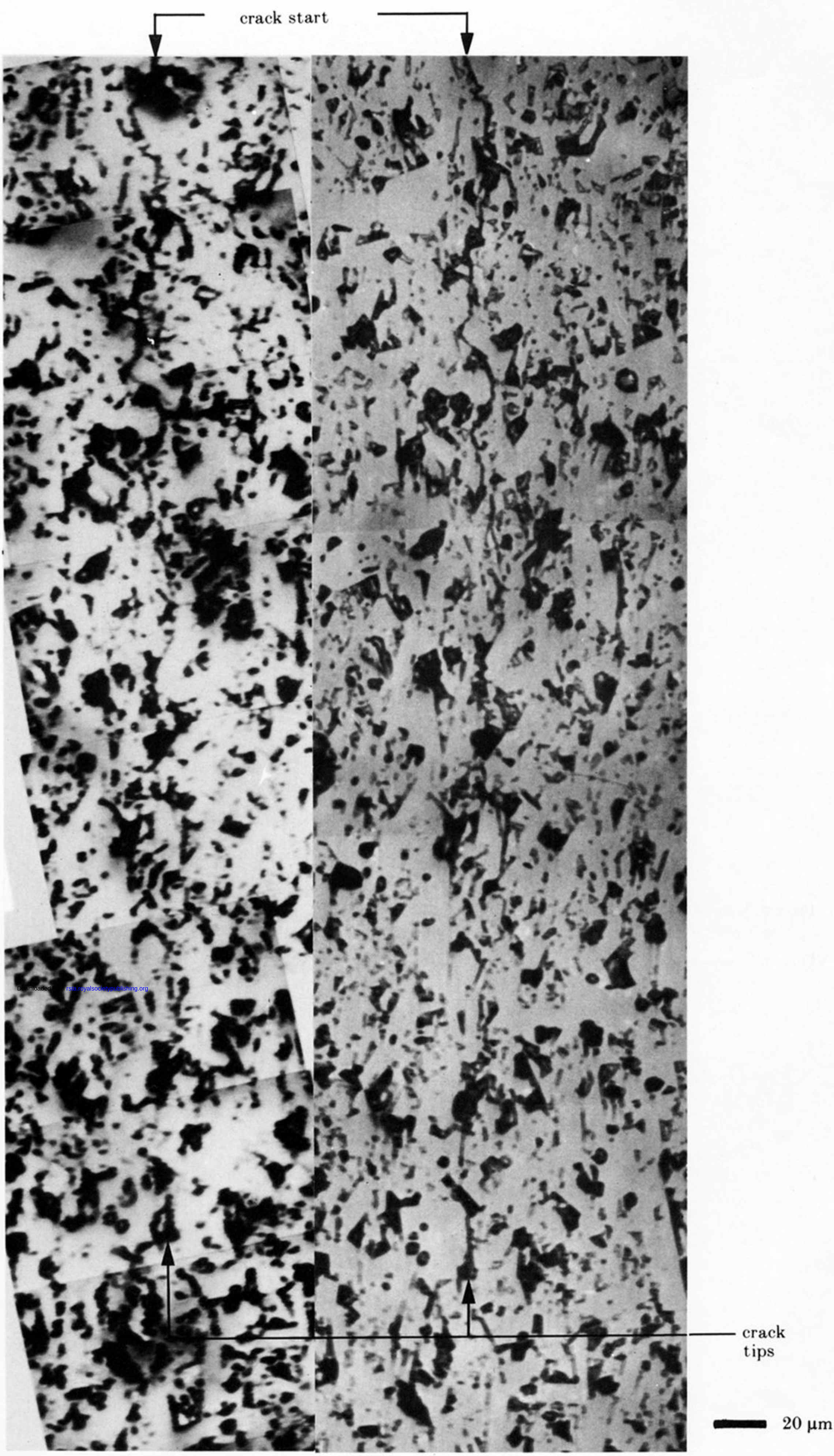

(*a*) (*b*)

FIGURE 5. (*a*) Composite acoustic image showing the main top surface crack from the indentation on sample B. (*b*) Composite optical image corresponding to the area of sample B shown in (*a*).

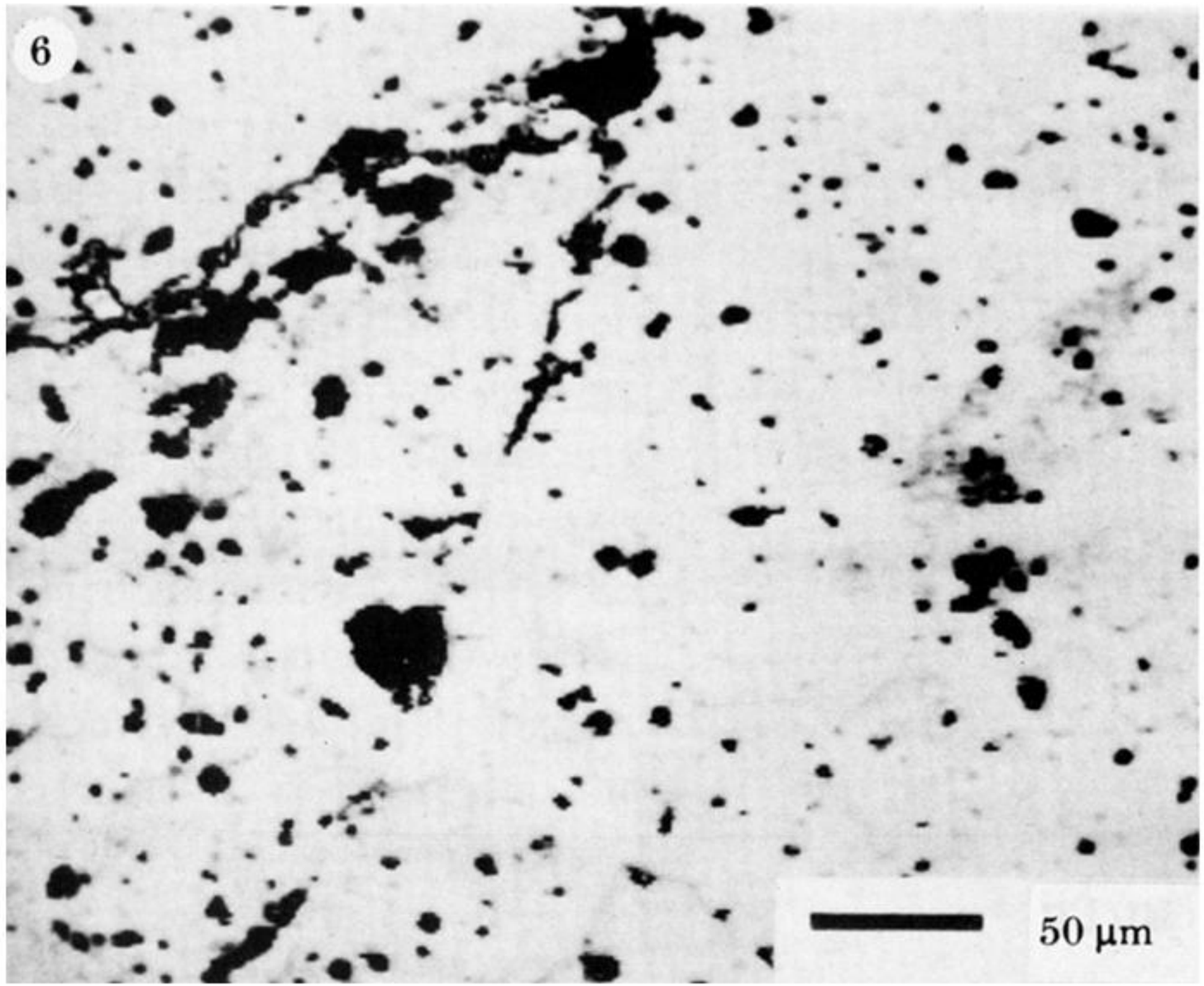

FIGURE 6. Acoustic image of the damage region of sample C showing a fine crack running diagonally from top right to lower left. Taken with the lens at focus ($z = 0$).

PHILOSOPHICAL TRANSACTIONS OF THE ROYAL SOCIETY A MATHEMATICAL, PHYSICAL & ENGINEERING SCIENCES

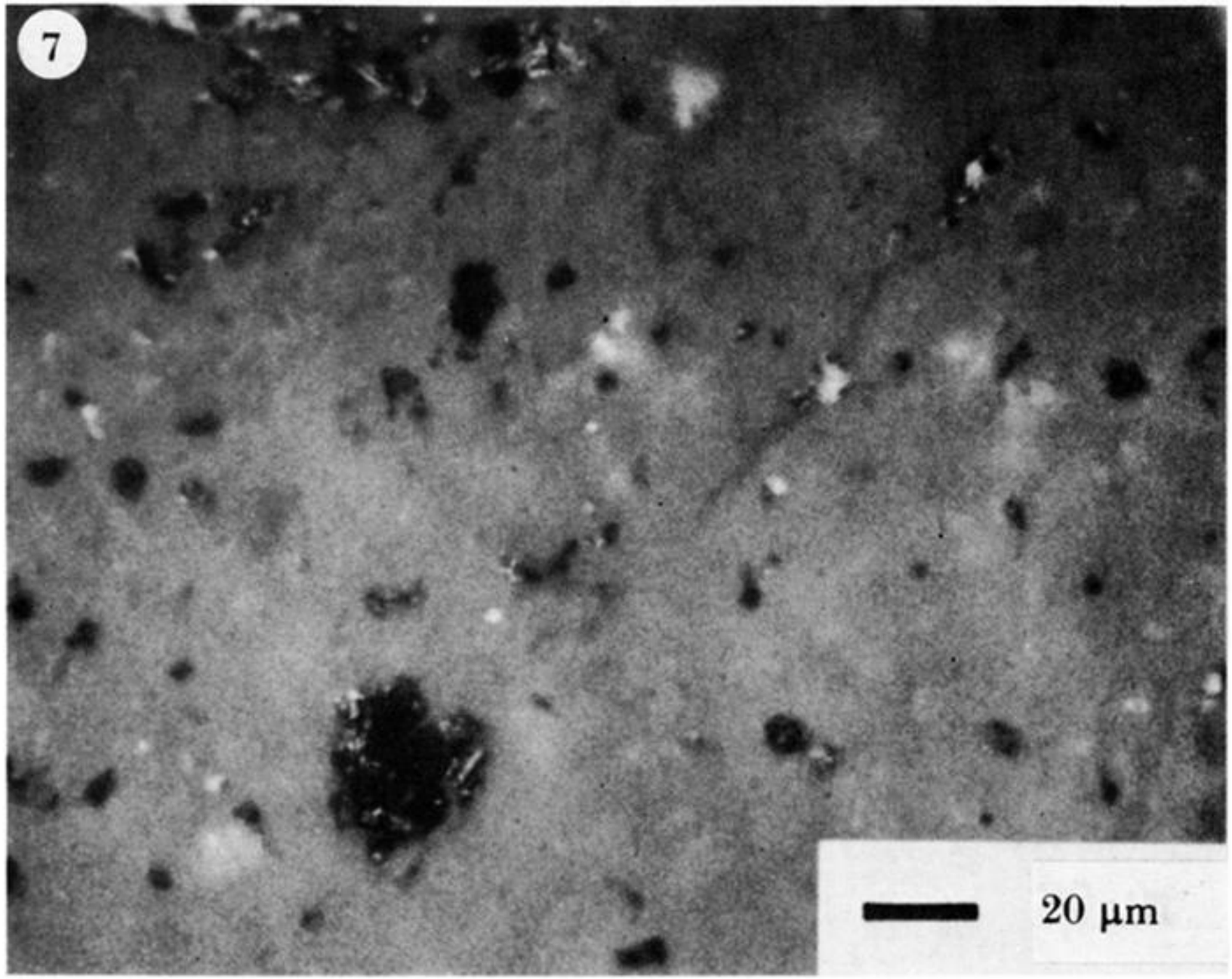

FIGURE 7. Optical image taken in reflection, corresponding to the area shown acoustically in figure 6.

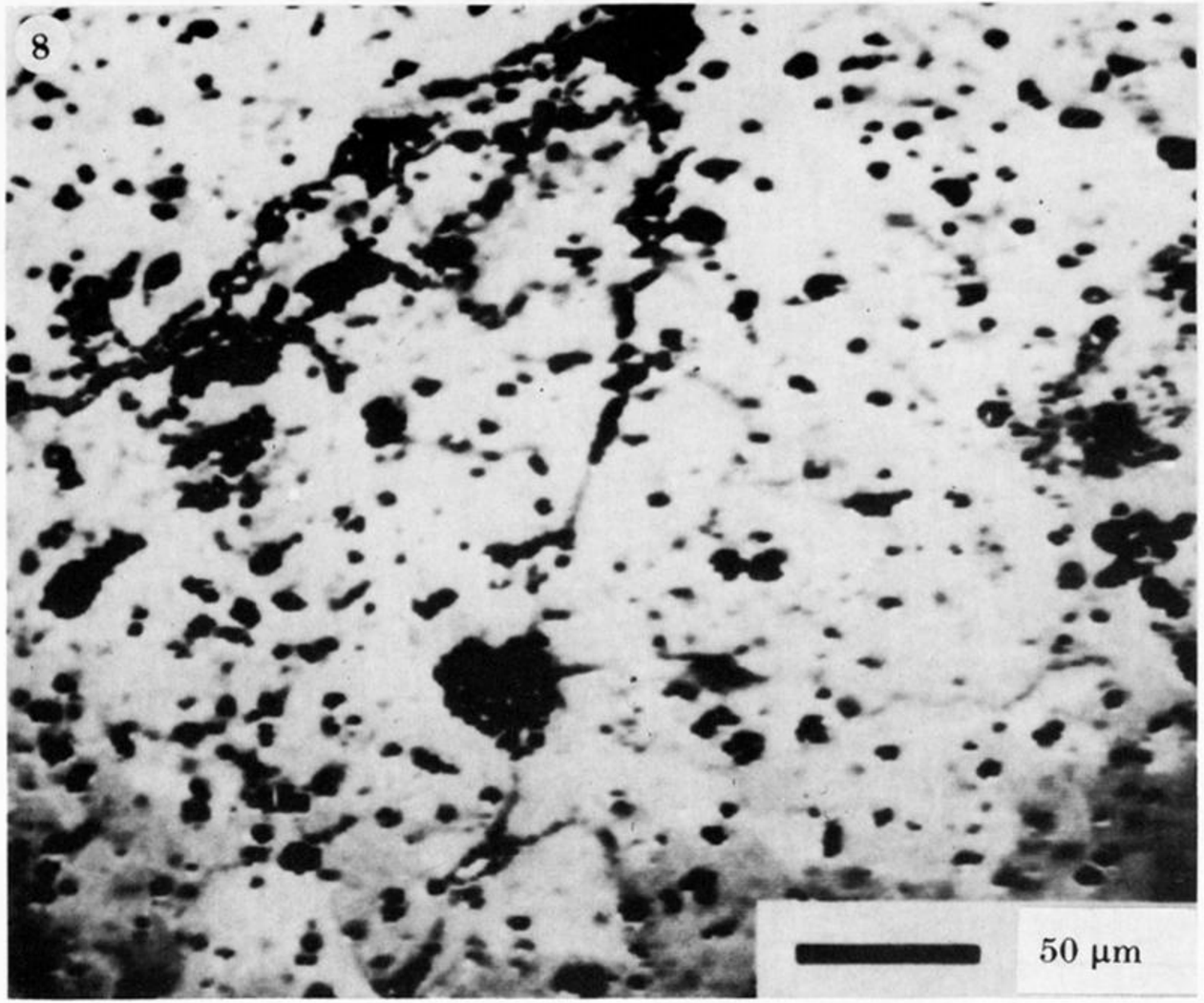

FIGURE 8. Acoustic image taken with $z = -5$ μm of defocus (lens moved 5 μm towards sample surface), corresponding to same area of sample C shown in figure 6.

PHILOSOPHICAL TRANSACTIONS OF THE ROYAL SOCIETY A MATHEMATICAL, PHYSICAL & ENGINEERING SCIENCES

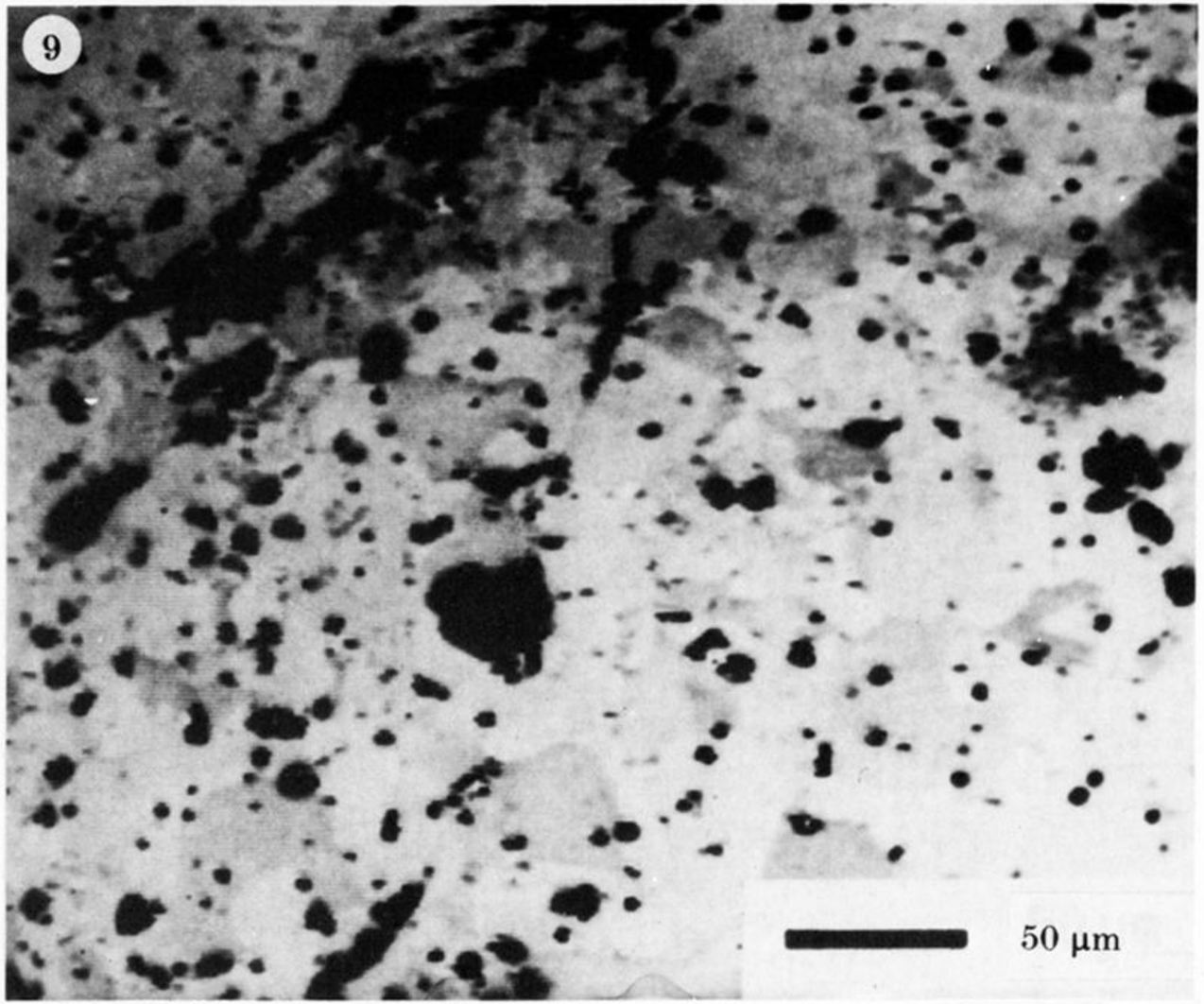

FIGURE 9. Acoustic image taken with $z = +5$ µm of defocus (lens moved 5 µm away from sample surface), corresponding to area of sample C showing in figure 6.

PHILOSOPHICAL TRANSACTIONS OF THE ROYAL SOCIETY A MATHEMATICAL, PHYSICAL & ENGINEERING SCIENCES

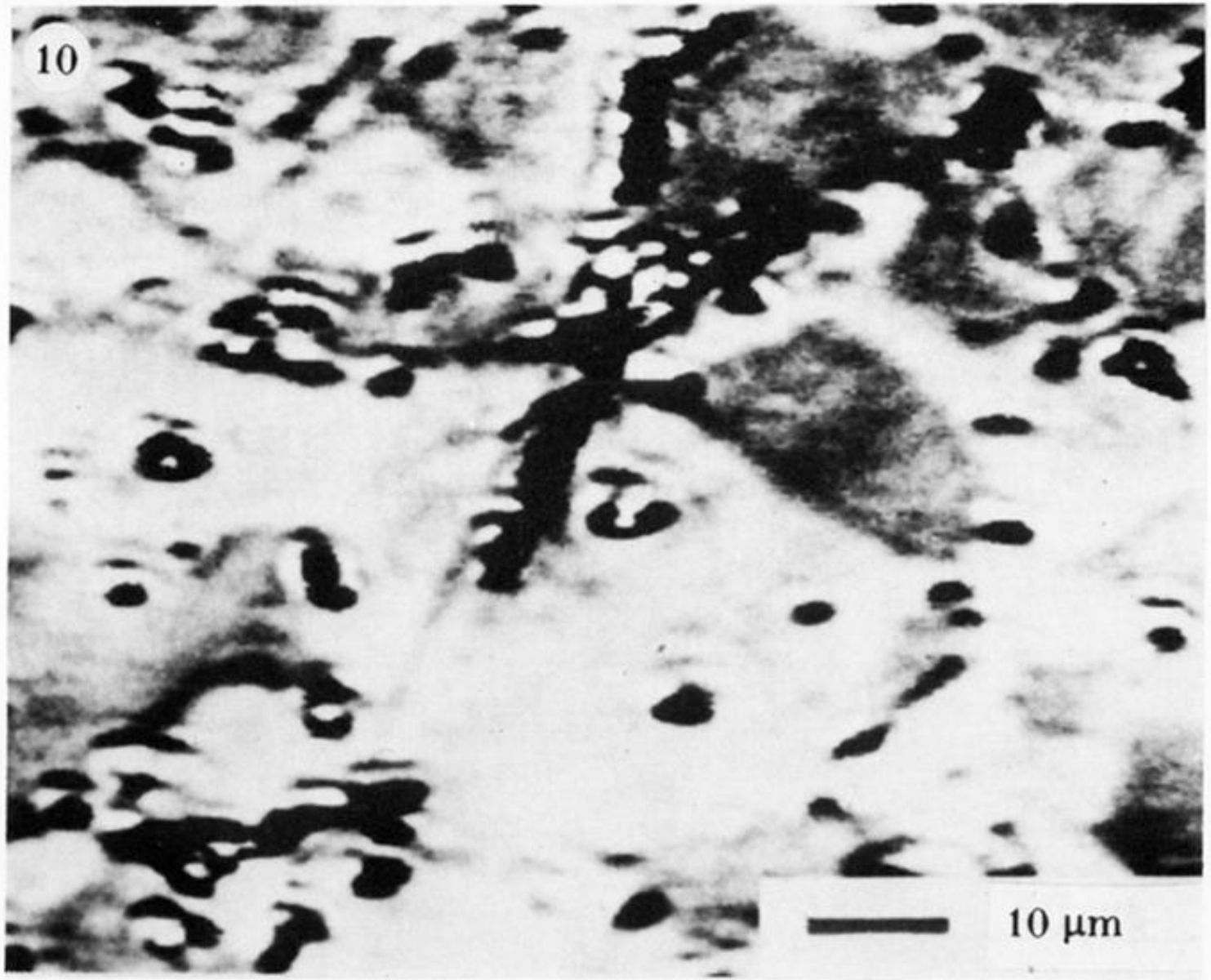

FIGURE 10. Acoustic image taken with $z = +8$ μm defocus of the central area of sample C shown in figure 6.

PHILOSOPHICAL TRANSACTIONS OF THE ROYAL SOCIETY A MATHEMATICAL, PHYSICAL & ENGINEERING SCIENCES